

Light management issues in intermediate band solar cells

Antonio Martí, Elisa Antolín, Enrique Cánovas, Pablo García Linares, and Antonio Luque
Instituto de Energía Solar - Universidad Politécnica de Madrid, ETSI Telecomunicación, Avda
Complutense 30, Madrid, 28040, Spain

ABSTRACT

This paper discusses several topics related to light management that improve our understanding of the performance and potential of the intermediate band solar cell (IBSC). These topics are photon recycling, photon selectivity and light confinement. It is found that neglecting photon recycling leads to underestimate the limiting efficiency of the IBSC in 7 points (56.1 % vs 63.2 %). Light trapping allows to effectively absorbing photons whose energy is associated to the weakest of the optical transitions in the IBSC, allowing also for higher efficiencies with lower device thickness. The impact of photon selectivity on the cell performance is also discussed.

INTRODUCTION

The intermediate band solar cell (IBSC) is a novel type of solar cell conceived to effectively use the energy of below bandgap energy photons [1, 2]. To this end, it requires the existence of an intermediate band (IB) located within the semiconductor bandgap (Fig. 1). This band divides the total bandgap of the semiconductor, E_G , into two sub-bandgaps, E_L and E_H . The IB is separated from the conduction and valence band (CB and VB) by a null density of states. Thanks to this band, two below bandgap energy photons, as those labelled “1” and “2” in Fig. 1 can create one electron–hole pair by pumping an electron from the VB to the IB (photon “1”) and an electron from the IB to the CB (photon “2”). To this end, in the classical IBSC model, the IB should be half–filled with electrons in order to provide both empty states to receive electrons from the VB as well as electrons to supply to the CB.

The IB material is sandwiched between conventional p and n type semiconductors. The region of IB material of interest is assumed to lay beyond the space charge region created by the junctions. When a voltage is applied, the null density of states between the IB and the CB and VB makes possible the appearance of three distinguished quasi-Fermi levels (E_{FC} , E_{FI} and E_{FV} , related each one to the conduction, intermediate and valence semiconductor bands respectively). The p and n regions (emitters) act as selective contacts and determine the position of the electron and hole quasi-Fermi levels (E_{FC} and E_{FV}). A sufficiently high density of states in the IB is assumed as to be able to keep E_{FI} at its equilibrium position [3]. As sketched in Fig. 1, the output voltage, V , determined by the quasi-Fermi level split between electrons and holes ($E_{FC} - E_{FV} = eV$) is still limited by the high bandgap E_G .

The complete details of the theory have been explained in detail in previous works [1, 2, 4, 5]. Experimental results related to the verification of the existence of three distinguished quasi-Fermi levels and absorption of two below bandgap energy photons can be found in Refs. [6, 7]. In this work, we will focus on advances related to our understanding of the role of light management in these cells.

INTERMEDIATE BAND SOLAR CELL MODEL

The limiting efficiency of the IBSC has been found to be 63.2 %. It has been calculated for the sun assumed as a black body at 6000 K and maximum concentration (46050 suns or $H_S=1/46050$ where H_S is the etendue per unit of cell area and when the refraction index of the

media in contact with the cell is air). The optimum gaps have been found to be $E_L=0.71$ eV, $E_H=1.24$ eV, $E_G=1.95$ eV [1, 2].

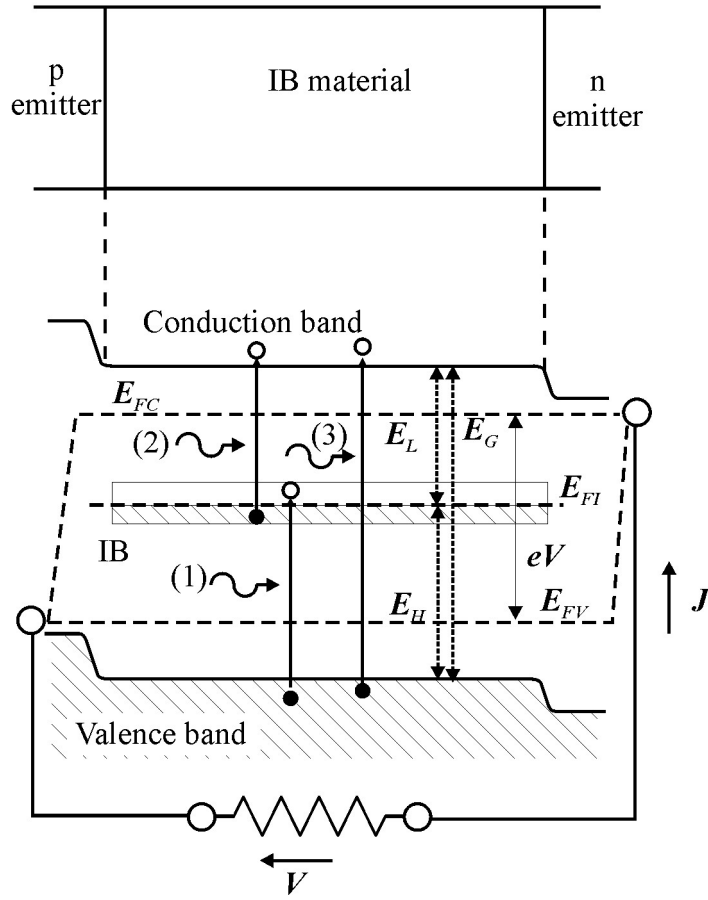


Figure 1. Simplified bandgap diagram under bias of an intermediate band solar cell indicating several magnitudes of interest such as quasi-Fermi energy levels ($E_{F,C}$, $E_{F,I}$ and $E_{F,V}$) and bandgaps (E_L , E_H and E_G). The top figure shows the correspondence of the bandgap diagram with the layer structure.

The model for the ideal current-voltage characteristic of an IBSC leading to this efficiency has been described elsewhere [1, 2, 4]. However, it is convenient to formulate the model again here adapted to facilitate the discussion of the specific light management phenomena that this paper will deal with.

For simplicity, a one-dimensional model (extending along the x direction defined by the unit vector u_x , Fig. 2) will be assumed for the IBSC. Hence, the following set of equations have to be satisfied for the electron (in the CB) and hole (in the VB) current densities (J_e and J_h) within the material sandwiched by the emitters and that contains the intermediate band:

$$-\frac{1}{e} \frac{dJ_e}{dx} = g_{ci} + g_{cv} - r_{ci} - r_{cv} \quad (1)$$

$$\frac{1}{e} \frac{dJ_h}{dx} = g_{iv} + g_{cv} - r_{iv} - r_{cv} \quad (2)$$

In these equations, e is the electron charge and g_{yz} and r_{yz} are the electron generation and recombination rates respectively between the y and z bands. When only radiative recombination is present, these rates are given by:

$$g_{yz} = \int \alpha_{yz} b_{\theta,\phi} d\epsilon d\Omega \quad (3)$$

$$r_{yz} = \int \alpha_{yz} b_n(\mu_{yz}) d\epsilon d\Omega \quad (4)$$

where: α_{yz} is the absorption coefficient related to optical transitions between band y and z ; $b_{\theta,\phi}$ is the spectral photon radiance (photon flux per unit of area, energy and solid angle Ω) along the direction \mathbf{u}_ξ characterised by forming an angle θ and ϕ with the unit vector along the x direction, \mathbf{u}_x (Fig. 2); $b_n(\mu_{yz})$ is the spectral photon radiance generated as a consequence of the radiative recombinations between bands y and z and is given by:

$$b_{yz} = \frac{2n^2}{h^3 c^2} \frac{\epsilon^2}{\exp\left(\frac{\epsilon - \mu_{yz}}{kT}\right) - 1} \quad (5)$$

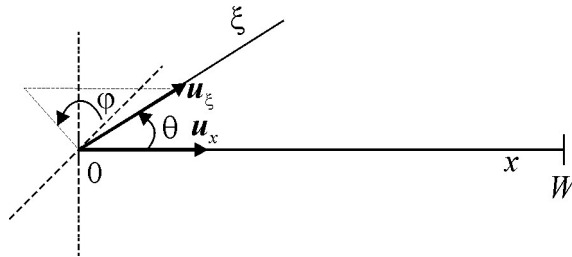


Figure 2. Drawing that allows to define the different angles and directions used in the description of the IBSC model.

In Eq. (5), n is the refraction index of the media, ε is the photon energy, h is the Planck's constant, c the speed of light in vacuum and μ_{yz} is the photon chemical potential which is equal to the difference between quasi-Fermi levels $E_{F,y}$ and $E_{F,z}$ ($\mu_{yz} = E_{F,y} - E_{F,z}$).

For the case in which the emitters are ideal and act only as selective contacts (that is, not recombining or generating carriers), $J_e(0)=0$, $J_h(W)=0$, being W the total thickness of the IB region, and the solution to Eqs. (1) and (2) is given by:

$$-J_e(W) = e \int (g_{ci} + g_{cv} - r_{ci} - r_{cv}) dx \quad (6)$$

$$-J_h(0) = e \int (g_{iv} + g_{cv} - r_{iv} - r_{cv}) dx \quad (7)$$

The current-voltage characteristic of the IBSC, J , with the sign criteria defined in Fig. 1 (positive when exiting the n emitter) is obtained from equalling Eqs. (6) and (7):

$$J = -J_e(W) = -J_h(0) \quad (8)$$

To count for the electric field and potential distribution in the IB region, the Poisson's equation should also be solved. However, in the ideal IBSC theory, the electronic density of states in the IB is assumed to be sufficiently large so that charge neutrality is automatically achieved by means of negligible shifts in the position of the intermediate band quasi-Fermi level (E_{FI}) with respect to its equilibrium position. Besides, since the IB is electrically isolated from the contacts by means of the p and n emitters, no electrical current flows through the intermediate band and therefore, the quasi-Fermi level E_{FI} remains flat also in non-equilibrium. This fact leads, since the bandgaps E_L and E_H are constant, to the fact that the conduction and valence bands also remain flat and therefore, to that the electric field is null in this region. In summary, under the hypothesis of sufficiently large density of states in the IB, we do not need to solve the Poisson equation since we know already its outcome.

In order to be able to count for the generation rate in Eq. (3) we need to calculate the spectral photon radiance $b_{\theta,\varphi}$. This radiance is dependent on the solar illumination but also, on photon recycling, that is, on the possibility that a photon being emitted as a consequence of a radiative recombination process is reabsorbed. Given the trajectory inside the cell defined by the unit vector \mathbf{u}_ξ and parameterized by ξ , the spectral photon radiance has to satisfy the following equation:

$$\frac{db_{\theta,\varphi}}{d\xi} = \alpha_{ci} b_n(\mu_{ci}) + \alpha_{iv} b_n(\mu_{iv}) + \alpha_{cv} b_n(\mu_{cv}) - (\alpha_{cv} + \alpha_{ci} + \alpha_{iv}) b_{\theta,\varphi} \quad (9)$$

Note that angles $\pi > \theta > \pi/2$ correspond to directions of propagation from the back towards the front of the cell. The boundary conditions for this equation depend on the optical properties, such as reflection, of the surfaces of the cell. Eqs. (1), (2) and (9) are coupled and difficult to solve in the general case. However, they can be integrated if the quasi-Fermi level splits μ_{yz} are

assumed constant. This is a reasonable assumption if the electron and hole mobility tends to infinity (not necessarily the carrier mobility at the intermediate band since, as mentioned, no carrier transport is assumed along the IB). Under this conditions, it is finally found [4] that:

$$J_e(0) = e \int M_e (F_{abs} - F_{em}) d\varepsilon - J_{B,e} \quad (10)$$

$$J_h(W) = e \int M_h (F_{abs} - F_{em}) d\varepsilon - J_{B,h} \quad (11)$$

The meaning of the factors M_e , M_h , $J_{b,e}$, $J_{b,h}$, F_{abs} , and F_{em} is collected in Table I. It is worthwhile mentioning for further discussion that F_{abs} , that represents the number of photons absorbed per unit of time and area, depends on the absorptivity of the cell, a . Unless otherwise stated, we will assume that a back reflector is located at the rear side of the cell ($x = W$) so that in this case:

$$a(\varepsilon) \approx 1 - \exp[-(\alpha_{cv} + \alpha_{ci} + \alpha_{iv})2W\kappa] \quad (12)$$

The utility of the factor κ appearing in the equation above will become apparent later. For the moment, it can be assumed that $\kappa = 1$ without further consideration.

Table I. Parameters involved in the calculation of the ideal current–voltage characteristic of an IBSC [4]. a is the absorptivity of the cell. T_S is the temperature of the sun (6000 K). T_C is the temperature of the cell (300 K).

<i>Etendue of the concentrated sunlight per unit of cell area; H_S</i>	
<i>Spectral photon flux absorbed by the cell;</i>	
$F_{abs} = H_S a F(\varepsilon, 0, T_S) + (\pi - H_S) a F(\varepsilon, 0, T_C)$	(T1-1)
<i>Spectral photon flux emitted by the cell;</i>	
$F_{emi} = \frac{\pi}{n^2} a \frac{\alpha_{cv} b_n(\mu_{cv}) + \alpha_{ci} b_n(\mu_{ci}) + \alpha_{iv} b_n(\mu_{iv})}{\alpha_{cv} + \alpha_{ci} + \alpha_{iv}}$	(T1-2)
<i>Auxiliary functions:</i>	
$M_e = \frac{\alpha_{cv} + \alpha_{ci}}{\alpha_{cv} + \alpha_{ci} + \alpha_{iv}}$	(T1-3)
$M_h = \frac{\alpha_{cv} + \alpha_{iv}}{\alpha_{cv} + \alpha_{ci} + \alpha_{iv}}$	(T1-4)
$J_{b,e} = e4\pi W \int R_{b,e} d\varepsilon$	(T1-5)
$J_{b,h} = e4\pi W \int R_{b,h} d\varepsilon$	(T1-6)
$R_{b,e} = \alpha_{cv} b_n(\mu_{cv}) + \alpha_{ci} b_n(\mu_{ci}) - M_e [\alpha_{cv} b_n(\mu_{cv}) + \alpha_{ci} b_n(\mu_{ci}) + \alpha_{iv} b_n(\mu_{iv})]$	(T1-7)
$R_{b,h} = \alpha_{cv} b_n(\mu_{cv}) + \alpha_{iv} b_n(\mu_{iv}) - M_h [\alpha_{cv} b_n(\mu_{cv}) + \alpha_{ci} b_n(\mu_{ci}) + \alpha_{iv} b_n(\mu_{iv})]$	(T1-8)
$F(\varepsilon, \mu, T) = \frac{2}{h^3 c^2} \frac{\varepsilon^2}{\exp\left(\frac{\varepsilon - \mu}{kT}\right) - 1}$	(T1-9)

THE ROLE OF PHOTON RECYCLING

In spite of the simplifications, the solution given by Eqs (10) and (11) consider the reabsorption of the photons that are emitted as a consequence of the radiative recombination processes (photon recycling, PR). This reabsorption is taken into account through the terms $\alpha_{yz}b_n(\mu_{yz})$ included in Eq. (9). (Perhaps it is not sufficiently known that photon recycling is also implicitly taken into account in the model that Shockley and Queisser [8] developed for calculating the limiting efficiency of single gap solar cells [9]).

Neglecting photon recycling effects is tentative since it notably would simplify obtaining a numerical (even analytical) solution for Eqs. (1) and (2) when quasi-Fermi levels are not constant (finite mobility) [10]. It can also be a reasonable assumption for those cases in which non-radiative recombination is expected to be dominant. In this respect, it will be illustrative to calculate the limiting efficiency of the IBSC concept if photon recycling is suppressed as a means to evaluate the impact of this phenomena in the IBSC performance. Note that suppressing PR is equivalent to make $\alpha_{ci}b_{ci} = \alpha_{iv}b_{iv} = \alpha_{cv}b_{cv} = 0$ in Eq. (9).

The current–voltage characteristic is then given by $J_e(0) = J_h(W)$ where:

$$J_e(0) = e \int M_e F_{abs} d\varepsilon - J_{B,e} \quad (13)$$

$$J_h(W) = e \int M_h F_{abs} d\varepsilon - J_{B,h} \quad (14)$$

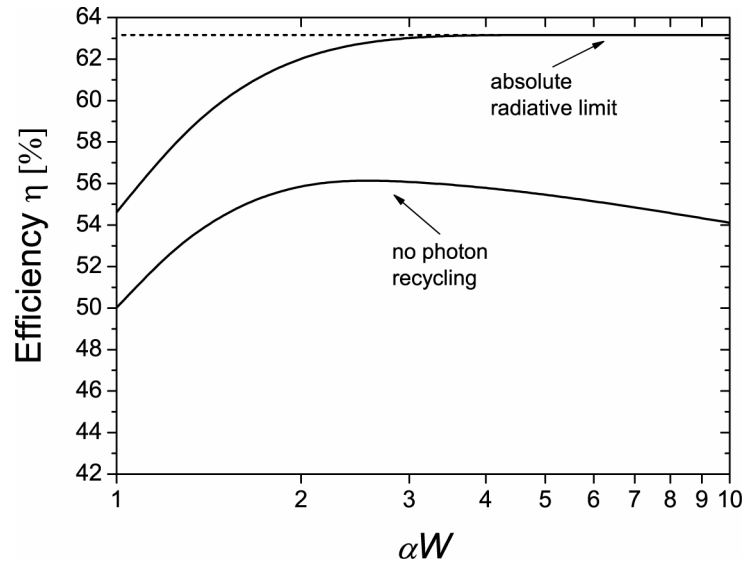


Figure 3. Efficiency of an ideal IBSC as a function of the thickness when considering and when neglecting photon recycling effects. For the calculations, the sun has been assumed as a black body at 6000 K. Maximum concentration (46050 suns) has been considered. Cell temperature is 300 K. The gaps of the IBSC are $E_L=0.71$ eV, $E_H = 1.24$ and $E_G = 1.95$ eV.

Fig. 3 plots the limiting efficiency of the IBSC as a function of the thickness of the cell, W , when taking into account PR [Eqs. (10) and (11)]. For this calculation, as previously mentioned, the bandgaps of the IBSC have been chosen to match the optimum ones, that is, $E_L=0.71$ eV, $E_H=1.24$ and $E_G=1.95$ eV. Besides, ideal photon selectivity for the absorption coefficients has been assumed. Photon selectivity means [11], that given a photon of energy ε , it can only be absorbed through a transition from the VB to the CB or from the VB to the IB or from the IB to the CB (Fig.4). Also, for this example, the strength of all the absorption coefficients has been assumed the same ($\alpha_{CV} = \alpha_{IV} = \alpha_{CI} = \alpha$). Notice then, that the figure 63.2 % is obtained when the thickness of the cell is sufficiently large so that $\alpha W \gg 1$ and therefore $a = 1$, that is, when the thickness of the device is sufficient to absorb all the incident photons.

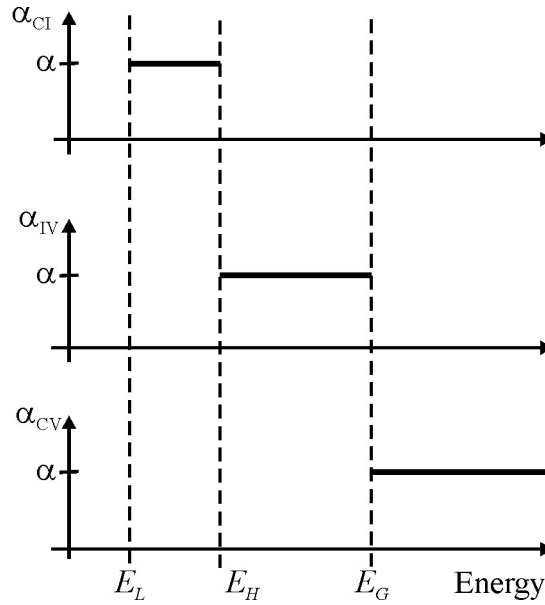


Figure 4. Simplified plot of the absorption coefficients involved in the operation of the IBSC when the conditions for ideal photon selectivity are met.

The limiting efficiency for this ideal IBSC, when neglecting PR effects [Eqs. (13) and (14)] is also plotted in Fig. 4 as a function of the thickness W . As a first observation, neglecting photon recycling reduces the limiting efficiency of the cell (from 63.2 % to 56.1 %). A kind of reduction was expected since, now that photons are not recycled, less photon energy is converted into electricity. On the other hand, it is found that the impact of PR in the efficiency of the cell is not negligible. Eventually, computational programs will have to be developed to model the performance of IBSCs that take into account PR as the performance of the cell approaches its radiative limit. It is also observed that when photon recycling is neglected, the efficiency decreases when increasing W beyond the point at which the maximum efficiency is achieved. This is also a common feature shared with conventional solar cells [9].

IMPACT OF PHOTON SELECTIVITY ON THE IBSC PERFORMANCE

Photon selectivity is also a figure of merit for the performance of the intermediate band solar cell. In terms of the absorption coefficients, it implies that, as represented in Fig. 5, the absorption coefficients do not overlap. When this is the case, Eqs. (10) and (11) reduce to:

$$J_e(0) = e \int (F_{abs} - F_{em}) d\varepsilon \quad (15)$$

$$J_h(W) = \int (F_{abs} - F_{em}) d\varepsilon \quad (16)$$

which become then the standard model used to calculate the limiting efficiency of IBSCs [1].

Photon selectivity could be regarded as a difficult condition to achieve. To study its impact on the limiting efficiency of the IBSC we will assume overlapping absorption coefficients exhibiting the general shape shown in Fig. 5. The shape assumed for the absorption coefficients implies increasing stepped strength of the absorption coefficient as the photon energy increases. When overlapping exists, for example, a photon with energy $\varepsilon > E_G$ can be absorbed by means of a transition from the VB to the CB but also from the VB to the IB and from the IB to CB. Besides, as before and for simplicity in the discussion of the results, we will assume that the absorption coefficients α_{yz} are constant above their energy absorption threshold.

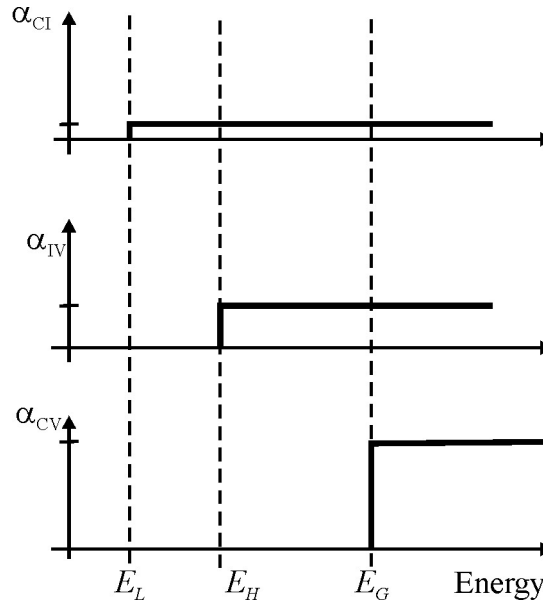


Figure 5. Simplified plot of the absorption coefficients involved in the operation of the IBSC when the conditions of ideal photon selectivity are not met.

As illustrative working case, we also will assume $\alpha_{CV} = 10\alpha_{IV} = 100\alpha_{CI}$. This choice is motivated by the hypothesis that, when implementing in practice the IBSC with quantum dots

(QDs) [12], the absorption coefficient that is associated to transitions from the confined states of the electrons in the dots to the conduction band continuum is the weakest of the absorption coefficients. This is also motivated by the poor overlapping between the wave function of the electron in the confined states and the conduction band continuum [13].

Fig. 6 represents the efficiency for this case of study as a function of $\alpha_{CI}W$. As it can be observed, the maximum efficiency is obtained for $\alpha_{CI}W \approx 1$ which physically implies, with the absorption model stated by Eq. (12), that the thickness of the cell is sufficiently thick as to allow almost complete absorption of photons with energy below E_L . Notice this absorption is necessary in order to have an effective transfer of electrons from the IB to the CB that complete the circuit [5] that allows the conversion of two below bandgap energy photons into one electron–hole pair.

It is also worthwhile noticing that, when overlapping exists between absorption coefficients, the efficiency again decreases when the thickness of the device is increased beyond the point for which its optimum value is achieved. This result is similar to the one that was obtained when photon recycling was neglected but it must be noticed that now, photon recycling is being taken into account. This results is then physically due to the fact that, when overlapping exists, the energy of the photons reemitted in radiative recombination processes (it will be remembered that in this case of study, all the recombination is radiative) is less effectively recycled when this overlap exists.

The observations in the paragraph above hints to the possibility that, by using light trapping techniques enhancing the optical path in the low photon energy range, devices with reduced thickness and enhanced efficiency could be used. To illustrate this potential we will consider a theoretical light trapping scheme in which the lowest energy photons ($\varepsilon < E_L$) would increase their optical path by a factor of 10. This feature can be implemented in our model by defining in Eq. (12) an energy dependent function, $\kappa(\varepsilon)$, so that:

$$\kappa(\varepsilon) = \begin{cases} 10 & \varepsilon < E_L \\ 1 & \text{elsewhere} \end{cases} \quad (17)$$

The efficiency limit in this case is illustrated again in Fig. 6. As it can be observed, the maximum efficiency is shifted towards a lower $\alpha_{CI}W$ value by a factor of 10. This is a logical consequence of the light trapping assumed by (17) since now, the same absorption of photons with energy $\varepsilon < E_L$ is possible with reduced thickness. Besides, a benefit in peak efficiency is obtained (from 56.7 % to 58.2 %). It is also worthwhile mentioning that, in the overlapping case, the limiting efficiency (63.2 %) is retaken as light trapping techniques are used that allow $W \rightarrow 0$ and

$$\alpha_{CV} = m\alpha_{IV} = m^2\alpha_{CI} \quad (18)$$

with $m \rightarrow \infty$ [4]. This will be, nevertheless, the case of study and discussion of the next section.

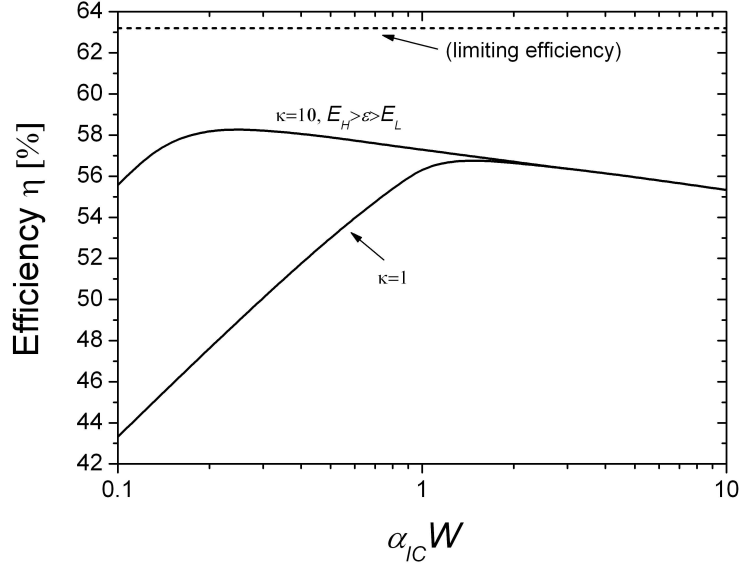


Figure 6. Efficiency of an IBSC as a function of its thickness and different light trapping conditions. The absorption coefficients have been assumed to overlap and have different strengths characterised by the factor $m=10$.

ANALYSIS OF THE IBSC EFFICIENCY AS A FUNCTION OF THE INTERMEDIATE BAND POSITION

In the ideal IBSC model represented by Eqs. (10) and (11) it can be easily checked that, when the IB is exactly located at the middle of the bandgap, the limiting efficiency of the IBSC is just that of the single gap solar cell made of the total bandgap E_G . This is due to the fact that, when the IB is located at the centre of the bandgap and ideal photon selectivity is assumed, the IB does not contribute to generate nor recombine electron-hole pairs (in the detailed balance radiative limit). It seems logical to think, however, that if we would allow to the intermediate band to contribute to the cell photocurrent when the IB is located at the centre of the bandgap we could still exceed the efficiency of the single gap solar cell made without intermediate band. We will study this case in the next paragraphs.

Eqs. (10) and (11), and the related implicit assumption of no overlapping between absorption coefficients, aim to determine the maximum efficiency of the IBSC but they do not imply that they lead to the maximum possible efficiency for any combination of bandgaps E_L and E_H and any value of the absorption coefficients.

To illustrate this, we can consider again the case in which the absorption coefficients overlap (Fig. 5). Under these circumstances, the IB located in the centre of the bandgap will now contribute to generate carriers from below bandgap photon absorption but a price will also have to be paid in recombination. The outcome of this balance, in terms of cell efficiency, is unclear at first sight and requires a direct calculation in order to elucidate. The results of this calculation are shown in Fig. 7 as a function of the IB position (E_L) for a cell of total bandgap 1.95 eV (the one leading to the 63.2 % limiting efficiency). The calculations have been carried according to the model described by Eqs (10)-(12) with $\kappa \rightarrow \infty$ (so that all the incoming photons are absorbed and

$a=1$) at the time that $W \rightarrow 0$ (light trapping). This framework will allow us to present the results independently of the device thickness and clarify the discussion while at the time results still represent an upper bound to the IBSC conversion efficiency when overlapping between absorption coefficients is considered. Different m factors in Eq. (18) have also been considered in the analysis.

The results show that for the intermediate band located in the centre of the bandgap and $m=1$, the limiting efficiency rises from 29.7% to 45.1%. This is a substantial increase, but still far from the IB full potential (63.2%). Moreover, as soon as m increases, the efficiency quickly increases and the optimum position of the IB shifts away from the centre of the bandgap. With $m=5$ the efficiency is already 58.8% and the optimum E_L has moved to 0.76 eV. The maximum efficiency progressively improves as m increases (as advanced in the previous section) until the limit of 63.2% for $E_L=0.71$ eV is regained.

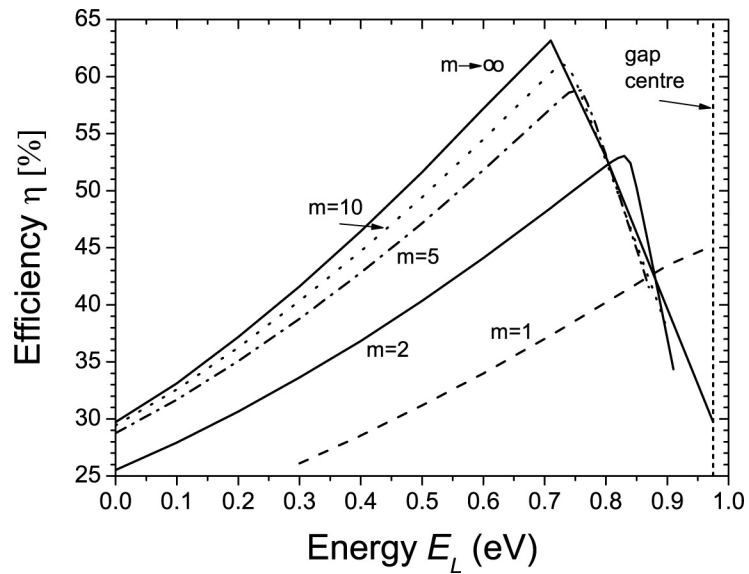


Figure 7. Efficiency of an IBSC as a function of the position of the intermediate band within the bandgap for several photon selectivity intensities (factor m). For the calculations, the sun has been assumed as a black body at 6000 K. Maximum concentration (46050 suns) has been considered. Cell temperature is 300 K. The total bandgap of the cell is $E_G = 1.95$ eV.

CONCLUSIONS

The ideal IBSC model takes into account photon recycling phenomena. In spite of their complexity, these phenomena can be analytically handled if the split between IBSC quasi-Fermi levels remains constant (this condition is achieved if infinite mobility conditions are approached). It has been calculated that neglecting photon recycling phenomena would lead to an underestimation of the IBSC limiting efficiency from 63.2% to 56.1%. It is anticipated that, as eventually IBSC are developed in practice, simulators that take into account this phenomena will

be needed to improve the IBSC designs as its operation becomes radiatively dominated and finite mobilities are considered.

The impact of removing the hypothesis of photon selectivity has also been included. When ideal photon selectivity conditions are not met, the efficiency of the IBSC decreases with respect to its theoretical maximum. The maximum is retaken if a large contrast between absorption coefficients exists and light trapping techniques are used to assist the transition that absorbs more weakly.

When the IB is located at the centre of the bandgap, the assumption of ideal photon selectivity does not lead to the maximum efficiency in the general case. However, the efficiency quickly improves and approaches its theoretical absolute maximum as the IB is shifted from the bandgap centre and ideal photon selectivity conditions are retaken.

ACKNOWLEDGMENTS

This work has been supported by the European Commission within the project FULLSPECTUM (SES6-CT-2003-502620) and the projects NUMANCIA (S-0505/ENE/000310) funded by the Comunidad de Madrid and GENESIS-FV (CSD2006-0004) funded by the Spanish National Programme. E.C acknowledges a "Plan Nacional de Formación de Personal Investigador" research grant.

REFERENCES

- [1] A. Luque and A. Martí, "Increasing the efficiency of ideal solar cells by photon induced transitions at intermediate levels," *Physical Review Letters*, vol. 78, pp. 5014–5017, 1997.
- [2] A. Luque and A. Martí, "A metallic intermediate band high efficiency solar cell," *Progress in Photovoltaics: Res. Appl.*, vol. 9, pp. 73–86, 2001.
- [3] A. Martí, L. Cuadra, and A. Luque, "Quantum dot analysis of the space charge region of intermediate band solar cell," in *Proc. of the 199th Electrochemical Society Meeting* Pennington: The Electrochemical Society, 2001, pp. 46-60.
- [4] L. Cuadra, A. Martí, and A. Luque, "Influence of the overlap between the absorption coefficients on the efficiency of the intermediate band solar cell," *IEEE Transactions on Electron Devices*, vol. 51, pp. 1002-1007, 2004.
- [5] A. Luque, A. Martí, C. Stanley, N. Lopez, L. Cuadra, D. Zhou, J. L. Pearson, and A. McKee, "General equivalent circuit for intermediate band devices: Potentials, currents and electroluminescence," *Journal of Applied Physics*, vol. 96, pp. 903-909, 2004.
- [6] A. Luque, A. Martí, N. Lopez, E. Antolín, E. Canovas, C. Stanley, C. Farmer, L. J. Caballero, L. Cuadra, and J. L. Balenzategui, "Experimental analysis of the quasi-Fermi level split in quantum dot intermediate-band solar cells," *Applied Physics Letters*, vol. 87, pp. 083505-3, 2005.

- [7] A. Martí, E. Antolin, C. R. Stanley, C. D. Farmer, N. Lopez, P. Diaz, E. Canovas, P. G. Linares, and A. Luque, "Production of Photocurrent due to Intermediate-to-Conduction-Band Transitions: A Demonstration of a Key Operating Principle of the Intermediate-Band Solar Cell," *Physical Review Letters*, vol. 97, pp. 247701-4, 2006.
- [8] W. Shockley and H. J. Queisser, "Detailed Balance Limit of Efficiency of p-n Junction Solar Cells," *Journal of Applied Physics*, vol. 32, pp. 510-519, 1961.
- [9] A. Martí, J. L. Balenzategui, and R. F. Reyna, "Photon recycling and Shockley's diode equation," *Journal of Applied Physics*, vol. 82, pp. 4067-4075, 1997.
- [10] A. Martí, L. Cuadra, and A. Luque, "Quasi drift-diffusion model for the quantum dot intermediate band solar cell," *IEEE Transactions on Electron Devices*, vol. 49, pp. 1632-1639, 2002.
- [11] A. S. Brown and M. A. Green, "Impurity photovoltaic effect: Fundamental energy conversion efficiency limits," *Journal of Applied Physics*, vol. 92, pp. 1329-1336, 2002.
- [12] A. Martí, L. Cuadra, and A. Luque, "Intermediate Band Solar Cells," in *NEXT GENERATION PHOTOVOLTAICS: High Efficiency through Full Spectrum Utilization*, A. Martí and A. Luque, Eds. Bristol: Institute of Physics Publishing, 2003, pp. 140-162.
- [13] A. Martí, C. R. Stanley, and A. Luque, "Intermediate Band Solar Cells (IBSC) using nanotechnology," in *Nanostructured Materials for Solar Energy Conversion* T. Soga, Ed.: Elsevier, 2006.